Green-synthesized silver nanoparticles using *Syzygium jambos* leaf extract: antioxidant, antibacterial, and potential therapeutic applications in functional foods

Mosleh Mohammad Abomughaid

Medical Laboratory Sciences Department, College of Applied Medical Sciences, University of Bisha, Bisha, Saudi Arabia

Corresponding Author: Mosleh Mohammad Abomughaid, Medical Laboratory Sciences Department, College of Applied Medical Sciences, University of Bisha, Bisha 67714, Saudi Arabia. Email: moslehali@ub.edu.sa

Academic Editor: Ismail Eş, PhD, Institute of Biomedical Engineering, Old Road Campus Research Building, University of Oxford, Headington, Oxford OX3 7DQ, UK

Received: 26 March 2025; Accepted: 14 July 2025; Published: 1 October 2025

ORIGINAL ARTICLE

Abstract

Food nanotechnology offers novel strategies for enhancing functional foods through bioactive delivery and antimicrobial protection. In this study, silver nanoparticles (AgNPs) were synthesized using *Syzygium jambos* leaf extract, which was confirmed by visual examination and ultraviolet-visible spectroscopy. Further characterization using Fourier transform-infrared spectroscopy, X-ray diffraction, scanning electron microscopy, energy dispersive X-ray spectroscopy, and transmission electron microscopy analysis identified the physicochemical properties of synthesized AgNPs, which displayed strong antioxidant potential, inhibiting 2,2-diphenyl-1-picrylhydrazyl and nitric oxide radicals in a dose-dependent manner. AgNPs also exhibited antibacterial activity against *Bacillus cereus* and *Shigella flexneri*, with zones of inhibition comparable to that of antibiotic control. However, zebrafish embryo toxicity studies revealed dose-responsive effects. These findings highlight *S. jambos*-mediated AgNPs as promising functional food additives with antimicrobial and antioxidant benefits, suitable for food preservation, disease sensing, and therapeutic delivery. Further safety evaluations are necessary for their integration into food and biomedical applications.

Keywords: silver nanoparticles; Syzygium jambos; antioxidant and antibacterial activity; zebrafish

Introduction

Nanotechnology considers nanoparticles (NPs) as advanced core material derived through the controlled atomic or molecular modification of bulk matter. Nanoparticles, typically ranging from 1 to 100 nanometers (nm), possess a high surface-to-volume ratio and enhanced chemical reactivity, which confer superior physicochemical and biological properties not observed in their bulk counterparts (Anbumani *et al.*, 2022). Recently, metal and metal-based nanoparticles—such as selenium, iron oxide, silver, gold, and platinum nanoparticles—have been extensively studied in the field of nanoscience because of their significant contributions to the diagnosis and treatment of life-threatening human diseases (Patel *et al.*, 2024; Priya *et al.*, 2017).

Silver nanoparticles (AgNPs) are gaining increasing attention because of their exceptional stability and superior biological, electrical, and optoelectronic properties, enabling their application across a wide range of sectors (Zhang *et al.*, 2016). Their antimicrobial and anti-inflammatory properties at varying dosages support their use in commercially available surgical bandages and dressings, where they help to accelerate wound healing. Additionally, the anti-infective quality of AgNPs makes

them suitable for use in biomedical implants, surgical instruments, and catheters (Jamkhande *et al.*, 2019). AgNPs also serve as active components in personal hygiene products such as toothpaste, bath gels, creams, ointments, and shampoos, functioning as biocidal agents (Pulit-Prociak *et al.*, 2019). Their unique characteristics enable a broad range of biomedical applications, including the development of novel therapeutics, biosensors, drug delivery systems, nutraceuticals, diagnostic tools, and bioimaging platforms (Jeevanandam *et al.,* 2022). Beyond biomedicine, AgNPs are also employed in environmental remediation, textiles, optoelectronics, energy generation, food packaging, and in the paint and ink industries. AgNPs exhibit diverse pharmacological properties, including antimicrobial, antiproliferative, virucidal, antiplatelet, anticoagulant, antifungal, antidiabetic, antibiofilm, and antioxidant activities (Dakshayani *et al.*, 2019; Khan *et al.*, 2023; Noppradit *et al.*, 2023; Tarannum and Gautam, 2019).

Owing to their versatile applications, various protocols have been developed to meet the demand for AgNPs. Physicochemical methods, such as spray pyrolysis, electrochemical techniques, ball milling, arc discharge, and laser ablation, are commonly employed for AgNP fabrication. Because these physical methods do not require chemical reducing agents (e.g., sodium citrate, sodium borohydride, or hydrazine), the resulting nanoparticles are typically pure and well-structured (Wei *et al.*, 2015). However, the requirement of high pressure and temperature, along with the associated costs, makes these methods less suitable for large-scale AgNP production. Additionally, the use of toxic chemical-reducing agents in chemical synthesis may pose risks in biomedical applications, as residual chemicals may adhere to nanoparticles and cause adverse health effects (Wang *et al.*, 2018).

The abundance, biodegradability, nontoxicity, and cost-effectiveness of biogenic protocols—using biological or native resources as bio-reducing agents or reaction media for synthesizing metal-based nanoparticles—have recently attracted significant interest from researchers as a sustainable alternative to conventional physicochemical methods (Kora and Rastogi, 2018). Green synthesis effectively addresses the issue of hazardous by-product generation commonly associated with traditional methods. Biological extracts derived from various plant parts (including stem bark, seeds, flowers, roots, leaves, and peels), as well as bacterial supernatants, fungi, macroalgae, and cyanobacteria, are widely utilized in the green synthesis of nanoparticles (Sonbol *et al.*, 2021).

Globally, antimicrobial resistance (AMR) is a rapidly escalating concern that urgently requires innovative strategies. The uncontrolled and excessive use of anti-infective drugs and antibiotics is a major contributor to the emergence of drug-resistant pathogenic bacterial strains (Alex *et al.*, 2024). Phyto-engineered nanoparticles have shown promising potential in combating multidrug-resistant (MDR) microbes through various mechanisms or via synergistic action when combined with conventional antibiotics, offering improved biocompatibility and biodegradability (Keshari *et al.,* 2020). Currently, nano-antibiotics—non-traditional antimicrobial agents synthesized from plant extracts—are widely explored as alternatives to conventional antibiotics and have garnered increasing attention from research groups globally (Huh and Kwon, 2011).

Extensive research is underway to design metallic nanoparticles using phytoextracts. Among these, plant extract-mediated synthesis of platinum, silver, and gold nanoparticles has demonstrated potent microbicidal activity against a broad range of microorganisms (Bordiwala, 2023; Chinnaraj *et al.,* 2023). The green synthesis of AgNPs using phytoextracts is particularly advantageous, as it is simple, rapid, cost-effective, and environmentally benign. Additionally, the biosynthesized AgNPs often exhibit defined morphology and size, achieved under optimized environmental conditions. These nanoparticles are well suited for biomedical applications because of their minimal or nontoxic disposition.

Green-synthesized AgNPs also demonstrate high yield, solubility, and stability (Jain *et al.*, 2021). Phytoconstituents, such as phenolics, ketones, tannins, flavonoids, ascorbic acid, phenols, amides, saponins, and terpenoids, contribute to both reduction of silver precursors and stabilization of the resulting nanoparticles (Kajani *et al.*, 2014). These phyto-derived compounds enhance the functional efficiency, stability, biocompatibility, and half-life of AgNPs (Arshad *et al.*, 2024). Various medicinal plant extracts are successfully employed in AgNP synthesis, including *Adhatoda vasica* leaf extract (Chaudhari *et al.*, 2023), *Calendula officinalis* seed extract (Baghizadeh *et al.*, 2015), *Zingiber officinale* root extract (Hu *et al.*, 2022), *Malva sylvestris* flower extract (Mahmoodi Esfanddarani *et al.*, 2018), *Trapa bispinosa* peel extract (Pandey *et al.*, 2013), *Phyllanthus emblica* (amla) fruit extract (Masum *et al.*, 2019), and stem extracts of *Entada spiralis* and *Piper chaba* (Mahiuddin *et al.*, 2020). AgNPs synthesized using these phytoextracts have shown multiple bioactivities, such as antibiofilm, antioxidant, antidiabetic, antifungal, anti-inflammatory, and antiproliferative effects (Ghojavand *et al.*, 2020).

Free radicals are generated as secondary products by living cells during essential aerobic metabolic processes. While low levels of free radicals play a vital role in maintaining immune function, excessive accumulation can lead to oxidative stress. Antioxidative compounds

enhance the activity of enzymes, such as glutathione peroxidase, superoxide dismutase, and catalase, or inhibit the expression of free radical-producing enzymes, such as nicotinamide adenine dinucleotide phosphate (NADPH) oxidase and xanthine oxidase (Chaudhary *et al.*, 2023). When the production of free radicals outweighs the body's antioxidant defenses, oxidative stress damages key macromolecules, including nucleic acids, lipids, and proteins. This imbalance contributes to the onset and progression of chronic degenerative diseases, such as rheumatoid arthritis, Parkinson's disease, diabetes mellitus, liver disorders, and cardiovascular conditions (Baskaran *et al.*, 2025; Dhandapani *et al.*, 2020). Natural compounds are a primary source of antioxidants. Phytochemicals—secondary metabolites produced by plants—play a beneficial role in regulating various cellular processes in the human body (Priya *et al.*, 2022). Nanoparticle formulations of plant-derived medications, often referred to as phyto nano-antioxidants, have shown enhanced therapeutic efficacy through improved antioxidant activity (Han *et al.*, 2022). Nanoparticles synthesized using plant extracts or active polyphenolic ingredients have demonstrated strong antioxidant properties, along with improved solubility, bioavailability, and targeted delivery (Balkrishna *et al.*, 2021). Among *in vivo* animal models, *Danio rerio* (zebrafish) is widely recognized as a cost-effective and reliable system for nanoparticle toxicity studies. Zebrafish share significant anatomical, genetic, and physiological similarities with humans. Their rapid development, small size, ease of maintenance, and transparent embryos make them ideal for real-time observation in toxicological research (Wehmas *et al.*, 2015).

Medicinal plants have long been used as natural healing agents in traditional medicine. The phytochemicals they contain possess both preventive and therapeutic potential against a variety of health conditions (Priya *et al.*, 2022; Uddin *et al.*, 2022).

The *Syzygium* genus, classified under the Myrtaceae family, includes nearly 3,000 species, all of which exhibit notable health benefits (Avila-Peña *et al.*, 2007). *Syzygium jambos* (commonly known as rose apple) is a small-to-medium size tree or shrub found in tropical regions globally. In traditional medicinal systems, various parts of the plant have been used to treat ulcers, hemorrhages, dental problems, respiratory disorders, leprosy, syphilis, and wounds. Leaf decoctions are traditionally used for treating eye infections and rheumatic conditions. Scientific studies have confirmed that the leaves and other plant parts of *S. jambos* exhibit antiurolithiatic, antibacterial, anti-inflammatory, anticancer, antioxidant, anticholinesterase, and antidiabetic properties (Rawa *et al.*, 2022). High flavonoid content found in most parts of the plant is largely responsible for its anti-inflammatory and antioxidant activities. Gallic acid, the principal phenolic acid in *S. jambos*, is distributed throughout the plant (Ochieng *et al.*, 2022) and may play a crucial role in reducing silver nitrate to form AgNPs. Previous studies have reported the successful synthesis of gold and AgNPs using leaf and bark extracts of *S. jambos*, primarily for antimalarial applications (Dutta *et al.*, 2017). Additionally, aqueous extracts from other *Syzygium* species, including *S. cumini*, *S. alternifolium*, and *S. aromaticum*, have been used for nanoparticle synthesis because of their strong reduction potential (Dhanislas *et al.*, 2023; Dutta *et al.*, 2017). Given its abundance and rich phytochemical profile, *S. jambos* presents itself as a promising candidate for green nanoparticle synthesis.

In this study, we focus on the green synthesis of AgNPs using *S. jambos* leaf extract and provide evidence of its reduction potential to produce uniform AgNPs. We further characterize the basic physicochemical properties of synthesized nanoparticles. Additionally, antibacterial and toxicity assessments offer foundational insights into their potential applications across biomedical and environmental domains.

Materials and Methods

Collection and preparation of the sample

The mature, healthy, and infection-free leaves of *S. jambos*, acquired from the local market in University of Bisha, Bisha, Saudi Arabia, were identified by a taxonomist, and specimen (voucher No. 09/2024) were stored at the University of Bisha, Bisha, Saudi Arabia. Three times washing of the leaves with tap water was executed to rule out detritus materials, and then the leaves were air-dried. Once the leaves were dried, these were finely powdered in a home mixer. To procure the aqueous leaf extract of *S. jambos*, exactly 5 g of leaf powder was mixed with 100 mL of distilled water in a sterile Erlenmeyer flask (200-mL capacity) placed on a hot plate with magnetic stirrer and boiled for 20 min at 60°C. The synthesized solution was filtered using a filter paper (Whatman No. 1) and light yellowish solution was carefully collected and retained for refrigeration (4°C) and used when needed for investigations.

Synthesis of AgNPs

The aqueous leaf extract of *S. jambos* was applied in the genesis of AgNPs. Briefly, in a sterile conical flask, exactly 10 mL of leaf aqueous extract was poured slowly into silver nitrate solution (1 mM, 100 mL), and stirred steadily for 30 min with a magnetic stirrer. After 24 h, a dark-brownish colored solution emerged, which was centrifuged (10,000 rpm) for 15 min. A dark brownish

pellet that appeared at the bottom of centrifuge tube was scrapped and redispersed thrice in distilled water to remove impurities. Purified AgNPs were air-dried and retained at 4°C for further analysis.

Spectroscopic and microscopic characterization

Ultraviolet-visible (UV-vis) spectral analysis

The UV-vis spectroscopic absorption investigation is a primary tool to characterize metallic nanoparticle's creation. The phyto-based reduction of silver ions by the secondary metabolic ingredients of *S. jambos* was checked. Exactly, 1 mL of the sample was poured in a sterile cuvette (quartz) and then the optical density from 200 nm to 800 nm (wavelength) was recorded.

Fourier transform-infrared spectroscopy (FTIR)

The specific functional groups of the leaf aqueous extract of *S. jambos* were identified using FTIR instrument. The vibrational frequencies developed in the spectra of FTIR discloses the phytoingredient's dynamic functional groups participation in the biological reduction, stabilization, and capping of metallic nanoparticles. The sample (2 mg) was amalgamated with potassium bromide (200 mg) and the pellet was designed. The pellet was scanned in the range of 500–4,000 cm^{-1} and the spectra were studied under ambient environment with specific resolution (4 cm^{-1}).

X-ray diffraction (XRD) analysis of AgNPs

To identify the crystalline trait and particle size of the AgNPs designed using *S. jambos* leaf aqueous extract, powder XRD was executed. The fabricated AgNPs were evenly layered on a microscopic sterile glass slide and the diffraction spectrum developed was captured in X-ray diffractometer. The diffractometer is functioned using 30 mA (current) and 40-kV voltage at 2θ range (20°–80° scanning mode) with λ = 1.54056 A° ("copper k alpha" [Cu kα] radiation). To compute the crystallite size of the designed AgNPs, Debye–Scherrer's equation was applied:

$$D = 0.94\,\lambda \div \beta \mathrm{Cos}\,\theta,$$

where D is the mean crystallite size of nanoparticles, λ is the X-ray radiation wavelength, β is full width at half maximum (FWHM) measure, and θ is the diffraction angle.

Scanning electron microscopy (SEM) with Energy dispersive X-ray (EDX)

The exterior features of the fabricated nanoparticles, such as morphology and dimension, were identified through SEM tool. The designed AgNPs were sonicated using distilled water and placed as a thin layer on a grid having carbon coating. The synthesized AgNPs were chemically analyzed for their elemental ingredient by using EDX analysis fitted with SEM tool.

Transmission electron microscopy (TEM)

Morphology along with the dimensional information of the designed AgNPs was achieved through TEM analysis. Sonication of AgNPs was conducted for 5 min in distilled water. On a copper-grid layered with carbon, a drop of nanoparticles was coated as a thin layer. With the aid of blotting paper, excess solution was wiped out and grid was air-dried for 10 min. Scanning was performed at different areas and the micrographic images was photographed.

2,2-Diphenyl-1-picrylhydrazyl (DPPH) assay

The DPPH radical scavenging methodology was applied to scrutinize the free radical quenching efficacy of the AgNPs synthesized applying *S. jambos* leaf aqueous extract. For the assay, DPPH (100 µM) was diluted in methanol (99.9%). Experiment was executed by amalgamating DPPH methanolic solution (3 mL) with 1-mL varying doses (25 µg/mL, 50 µg/mL, 75 µg/mL, 100 µg/mL, and 125 µg/mL) of AgNPs. The synthesized mixture was retained to react for 30 min in a dark environment at ambient conditions (37°C) and optical density (OD) was observed spectrophotometrically (517 nm). Ascorbic acid (as a standard positive control) and methanol (as a blank solution) were used. The percentage DPPH inhibition was computed by applying the following equation:

$$\%\ \text{Inhibition of DPPH} = \frac{AB_C - AB_S}{AB_C} \times 100,$$

where AB_C is the control absorbance, and AB_S is the AgNPs absorbance.

Nitric oxide (NO) assay

To evaluate the NO scavenging efficacy of the AgNPs designed using aqueous leaf extract of *S. jambos*, a published protocol with mild amendment was employed (Borquaye *et al.*, 2020). Precisely, 2 mL of 10-mM sodium nitroprusside, 0.5 mL of phosphate buffer solution (PBS), and 0.5 mL of test samples of varying doses (25 µg/mL, 50 µg/mL, 75 µg/mL, 100 µg/mL, and 125 µg/mL) were blended in a sterile test tube. Incubation of the reacting mixture was performed for 150 min at 25°C. To the incubated reaction solution (0.5 mL), 30% of 1-mL sulphanilamide, made using glacial acetic acid, was poured and retained for 5 min. Re-incubation of the reaction solution was performed for 30 min at 25°C, after the addition of 1 mL of 0.1% w/v napthylethylenediamine dihydrochloride (NED). A pinkish color appeared from the diazotization reaction between nitrite ions and sulfanilamide; conjugation with NED was observed at 540 nm through spectrophotometer. In a similar manner, standard solution (ascorbic acid) was prepared. For bank solution, the

S. jambos leaf aqueous extract was replaced by ethanol. The inhibitory percentage of NO radicals was computed by using the following equation:

$$\% \text{ of NO inhibition} = \frac{AB_C - AB_S}{AB_C} \times 100,$$

where AB_C is the control absorbance, and AB_S is the AgNPs absorbance.

Well-diffusion methodology for antibacterial assay

As per the published methodology of Ragunathan *et al.* (2022), with milder alterations, the antibacterial performance of the AgNPs designed from the *S. jambos* aqueous leaf extract was checked for two infective bacterial strains: *Bacillus cereus*/*B. cereus* and *Shigella flexneri*/*S. flexneri*. Agar-well diffusion methodology using Mueller–Hinton (MH) agar media was performed. The freshly made MH agar media was gently poured into petri-plates and waited for solidification in a laminar airflow (LAF) chamber to restrict contamination. Using 100 µL of bacterial culture, each petri-plate was swabbed individually. The wells were designed using steel well borer (3 mm). Then, 10 µL of AgNPs of varying doses (20 µg/mL, 30 µg/mL, 40 µg/mL, and 50 µg/mL) were poured into the agar-well and the plated AgNPs were retained for a day at ambient conditions (37°C) in a bacterial incubator. Exactly, 10 µg/mL of ciprofloxacin (antibiotic) was applied as a standard/positive reference drug. Inhibition zones that emerged around all the wells in each petri-plate were measured in millimetres (mm).

Zebrafish embryo toxicity assay

To assess the toxicity impact of the fabricated AgNPs on the embryonic zebrafish, the protocol experimented by Ganeshkumar *et al.* (2012) with slight amendment was performed. Through spawning, the egg of the zebrafish was collected and retained for embryo formation. Healthier embryos (eight-cell stage) of zebrafish were collected, washed thrice with distilled water, and preserved in a petri-plate. In a 24-well microtiter plate, 20 zebrafish embryos were placed in each well. The embryos were reacted with varying doses (100 µg/mL, 200 µg/mL, and 300 µg/mL) of *S. jambos* aqueous leaf extract-fabricated AgNPs and incubated at three varying intervals (24, 48, and 72 h). All the procedures were carried out strictly with institutional and national guidelines for the care and use of fisheries. This study was approved by the Animal Ethics Committee at University of Bisha (UB-H-03/23).

Statistical analysis

All the protocols were performed for three times (n = 3) and the data were collected as means ± SD. Paired test statistical analysis was carried out wherever required. The GraphPad Prism software (version 6) was employed for determining the half-maximal inhibitory concentrations (IC_{50}), and the graphs were illustrated.

Results

Visual investigation and UV analysis

The yellow color *S. jambos* leaf aqueous extract when amalgamated with NO aqueous solution swiftly turned to dark-brownish color within 10 min. The dark-brownish color intensity deepens with increase in retention period, reflecting direct proportionality. The appeared dark-brownish color was the basic hallmark for the genesis of AgNPs after 24 h of retention at ambient conditions. The fabricated AgNPs evinced a specific intensive peak at 420 nm when assessed through UV-vis spectrophotometer. This was due to surface plasmon resonance (SPR) of AgNPs and ranged almost from 350 nm to 480 nm (Figure 1). The purity of the synthesized nanoparticles was observed from the result. Despite the washing steps, there was a peak at 250 nm, which signified the presence of phenolic acid and flavonoids present in the plant extract.

FTIR

Applying the FTIR tool, the bioactive ingredients of the aqueous leaf extract of *S. jambos*, engaged in the

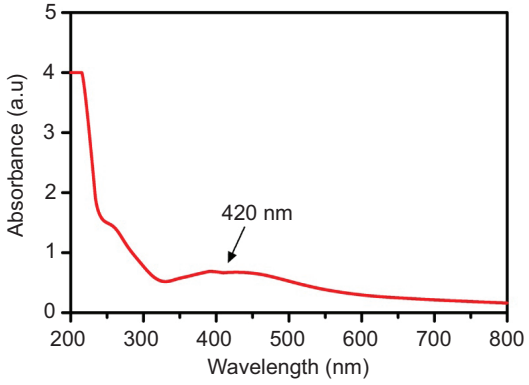

Figure 1. The UV-visible absorption spectrum of AgNPs synthesized using *S. jambos* leaf aqueous extract. A prominent surface plasmon resonance peak was observed at 420 nm, confirming AgNP formation. The absorption band between 350 nm and 480 nm supports the colloidal nature of the nanoparticles, while a minor peak near 250 nm indicates the presence of phytochemicals, such as phenolic acids and flavonoids, adsorbed on surface of the nanoparticles. Spectra were recorded between 200 nm and 800 nm using quartz cuvettes after 24-h incubation at room temperature.

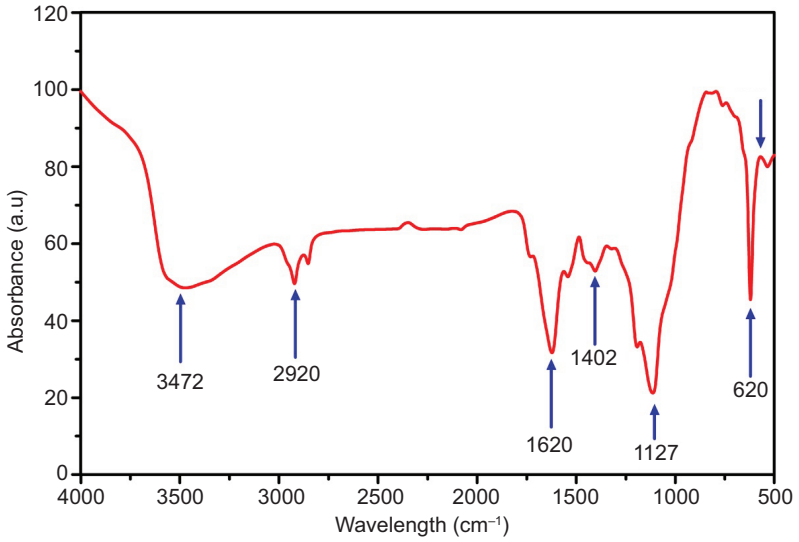

Figure 2. The FTIR spectrum of AgNPs synthesized using *S. jambos* leaf aqueous extract recorded in the range of 500–4000 cm^{-1} with a resolution of 4 cm^{-1} under ambient conditions. Distinct peaks observed at 3,472 cm^{-1} (O-H stretching of alcohols/phenols), 2,920 cm^{-1} (C-H stretching of methyl groups), and 1,620 cm^{-1} (C=O or C-O stretching of flavonoids) indicate the involvement of phytochemicals in the reduction, stabilization, and capping of AgNPs.

bio-based reduction, stabilization as well as capping of AgNPs, were revealed (Figure 2). A peak formed at 3,472 cm^{-1} demonstrated the O-H stretch of the alcoholic/phenolic ingredients of *S. jambos* leaf extract. For flavonoid's C-O stretch, a peak was discovered at 1,620 cm^{-1}. A peak for the methyl group's C-H stretch was formed at 2,920 cm^{-1}.

XRD spectral pattern of AgNPs designed from *S. jambos* leaf aqueous extract

The XRD was conducted to discover the crystalline quality as well as crystallite size of fabricated AgNPs. The diffraction pattern of peak developed at 2θ with the hkl plane values (Miller indices) as 38.90° (111), 44.91° (200), 64.34° (220), and 77.29° (311), as shown in Figure 3. This diffraction spectrum dictated the face-centered cubic (fcc) of AgNPs with crystallinity. Moreover, the spectra matched with the Joint Committee on Powder Diffraction Standards (JCPDS) file No. 04-0783. The AgNPs were spheroidal in morphology. The mean grain size (particle size) of the AgNPs, calculated using Debye–Scherrer equation, was 17.80 nm.

SEM analysis

The exterior morphology of the fabricated AgNPs was projected through the SEM micrographic images presenting spheroidal nanoparticle's shape along with aggregation (Figure 4). Similitude to the present report, the AgNPs acquired using *Salvia officinalis* also dictated spheroidal morphology, in addition to agglomeration.

EDX analysis

The EDX spectra that appeared from 2.5 kiloelectron volt (keV) to 4 keV was specific for AgNPs (Figure 5). The spectra showed that the fabricated AgNPs owned 45.95% silver, 22.80% oxygen, and 33.27% carbon. Carbon existence in the spectra might be from the SEM grid, and the oxygen atom was contributed by the phytometabolites leaf aqueous extract of *S. jambos*. Similar form of outcomes is found in the literature.

TEM analysis

The micrographic image of TEM provided spheroidal shape and smooth edged nanoparticles having a dimensional range of 12–25 nm and a mean size of 18.9 nm (Figure 6). The synthesized AgNPs also revealed a layer of phytocomponents at the edge of nanoparticles. This prescribed the major activity of the aqueous leaf extract of *S. jambos* in the various phases of nanoparticle's synthesis.

DPPH assay

The DPPH radical quenching impact of *S. jambos* leaf aqueous extract-fabricated AgNPs was assessed. The AgNPs showed suppression in DPPH radical with the

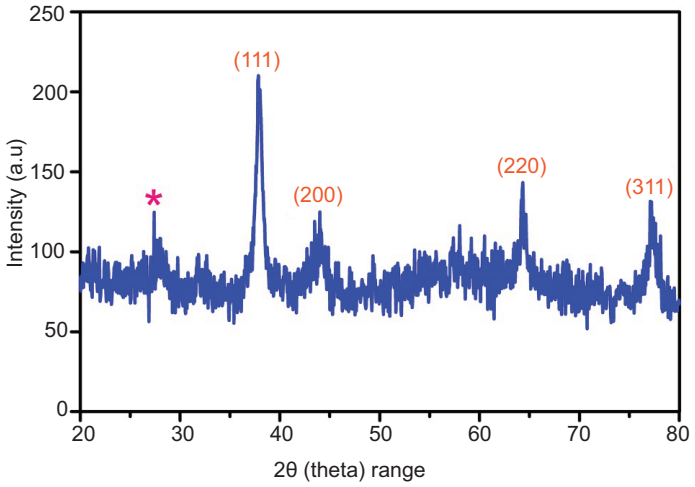

Figure 3. The XRD pattern of AgNPs synthesized using *S. jambos* leaf aqueous extract, scanned over a 2θ range of 20°–80° using Cu kα radiation (λ = 1.54056 Å). The diffraction peaks observed at 38.90°, 44.91°, 64.34°, and 77.29° matched with the (111), (200), (220), and (311) planes of fcc silver, respectively, consistent with the JCPDS file No. 04-0783. The average crystallite size, calculated using the Debye–Scherrer equation, was approximately 17.8 nm.

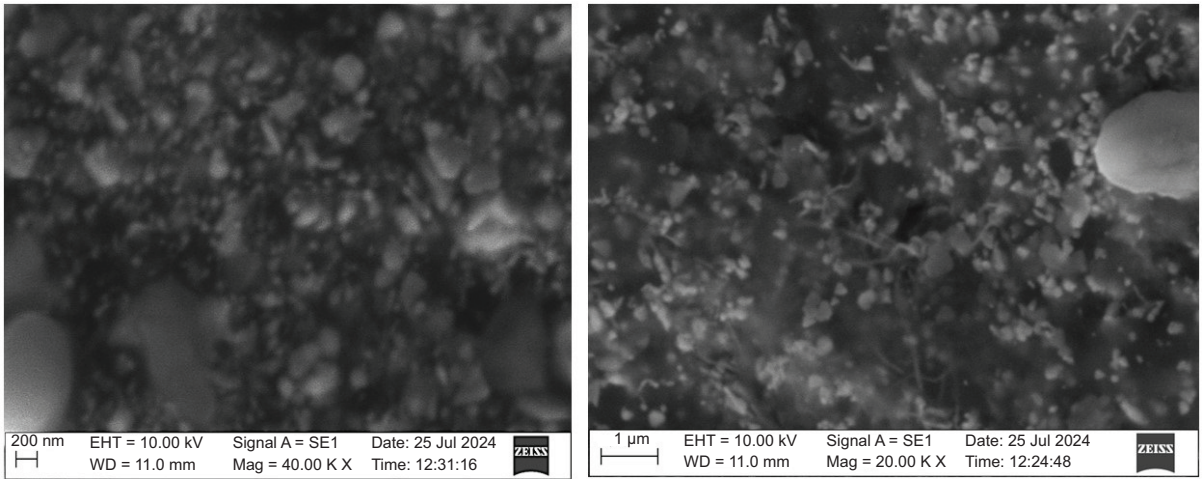

Figure 4. The SEM images of AgNPs synthesized using *S. jambos* leaf aqueous extract captured at two different magnifications. The images reveal predominantly spherical morphology with moderate agglomeration and relatively uniform particle distribution. Samples were sonicated in distilled water and deposited on a carbon-coated grid prior to imaging.

inhibitory proportion of 19.29–79.02% when screened from 25 µg/mL to 125 µg/mL. The inhibitory activity escalated with an upsurge in the concentration of AgNPs. Similarly, the standard positive control (ascorbic acid) displayed escalated percentage inhibition of DPPH radical (26.02–82.82%) (Figure 7). The IC_{50} doses for AgNPs and ascorbic acid were computed as 88.76 µg/mL and 86.37 µg/mL, respectively.

Nitric oxide scavenging assay

The NO scavenging assay was conducted to display the anti-radical efficacy of the AgNPs acquired from *S. jambos* aqueous leaf extract. At the lowest experimented dose of AgNPs (25 µg/mL), the inhibition of NO was 23.82%, and at maximum dose (125 µg/mL), 65.38% was the NO inhibition. The inhibitory performance of AgNPs toward the NO radical was entirely dose-based. As the concentration escalated, the inhibitory percentage also increased with an IC_{50} of 68.34 µg/mL. Similarly, ascorbic acid also showed an escalated inhibitory proportion of 27.87–75.69% with an IC_{50} dose of 66.67 µg/mL (Figure 8).

Antibacterial activity

The antibacterial efficacy of the AgNPs designed by applying *S. jambos* aqueous leaf extract was analyzed. Gram-positive and Gram-negative strains of bacteria

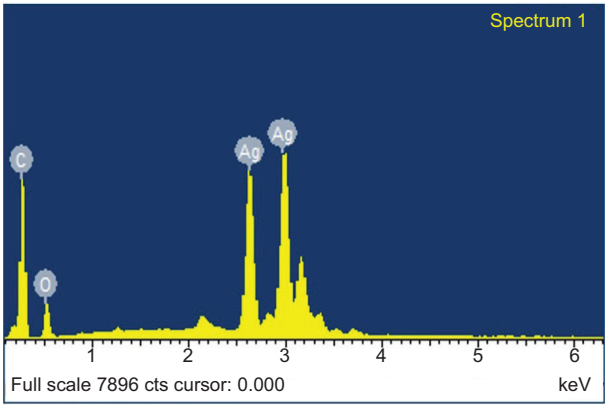

Figure 5. The EDX signal of AgNPs synthesized using *S. jambos* leaf aqueous extract. A strong characteristic silver signal is observed between 2.5 keV and 4 keV, confirming the elemental composition of AgNPs. The spectrum indicated 45.95% silver, 33.27% carbon (attributed to the carbon-coated SEM grid), and 22.80% oxygen, probably originating from the phytochemicals capping the surface of nanoparticles.

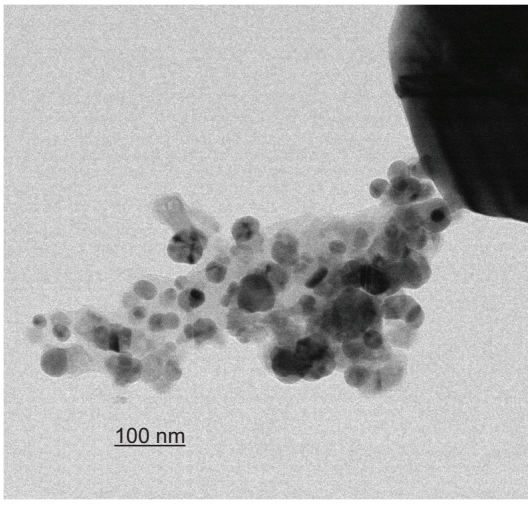

Figure 6. The TEM micrographs of AgNPs, synthesized using *S. jambos* leaf aqueous extract, show spherical nanoparticles. The micrographs reveal predominantly spherical nanoparticles with smooth edges, exhibiting size ranging from 12 nm to 25 nm and an average diameter of approximately 18.9 nm. A thin layer of phytochemical capping is visible around nanoparticles, indicating the role of plant metabolites in stabilization. Scale bar represents 100 nm.

were used. The AgNPs demonstrated strong antibacterial activity against each bacterium with visible inhibitory zone. The diameter of inhibitory zone increased with increased dose of AgNPs. The antibacterial activity was observed to be dose-dependent. At a maximum dose (50 µg/mL) of AgNPs, the inhibitory zone of *Bacillus cereus* was 10.3 ± 0.62 mm, whereas for *Shigella flexneri*, the

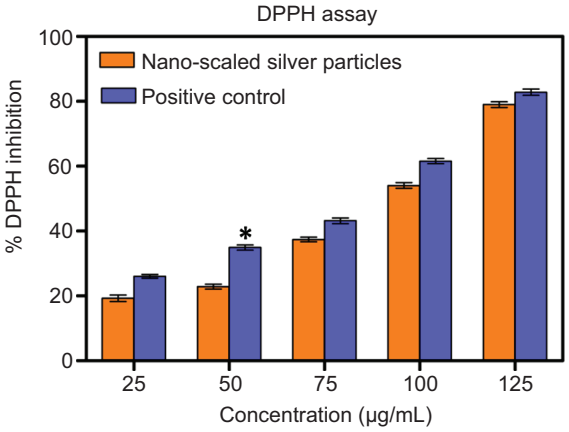

Figure 7. The dose-dependent DPPH radical scavenging activity of AgNPs synthesized using *S. jambos* leaf aqueous extract, compared to ascorbic acid as a positive control. The inhibitory effect increased with AgNP concentration from 25 µg/mL to 125 µg/mL, reaching a maximum inhibition of 79.02%, close to ascorbic acid's 82.82%. IC_{50} values were 88.76 µg/mL for AgNPs and 86.37 µg/mL for ascorbic acid. Data represent mean ± SD; and *indicates statistical significance versus control ($P < 0.05$).

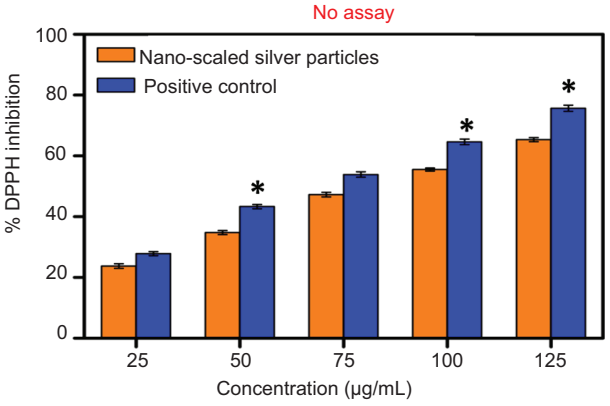

Figure 8. The dose-dependent NO radical scavenging activity of AgNPs synthesized using *S. jambos* leaf aqueous extract, compared to ascorbic acid as a positive control. The AgNPs showed increasing NO inhibition from 23.82% to 65.38% across concentration of 25–125 µg/mL, with an IC_{50} of 68.34 µg/mL. Ascorbic acid exhibited inhibition from 27.87% to 75.69%, with an IC_{50} of 66.67 µg/mL. Data represent mean ± SD; and * indicates statistical significance versus control ($P < 0.05$).

inhibitory zone was 8.0 ± 0.40 mm. The acquired outcomes are displayed in Table 1 and Figure 9.

Zebrafish embryo cytotoxicity study

The toxic nature of AgNPs synthesized using *S. jambos* leaf aqueous extract was assessed on the formation and

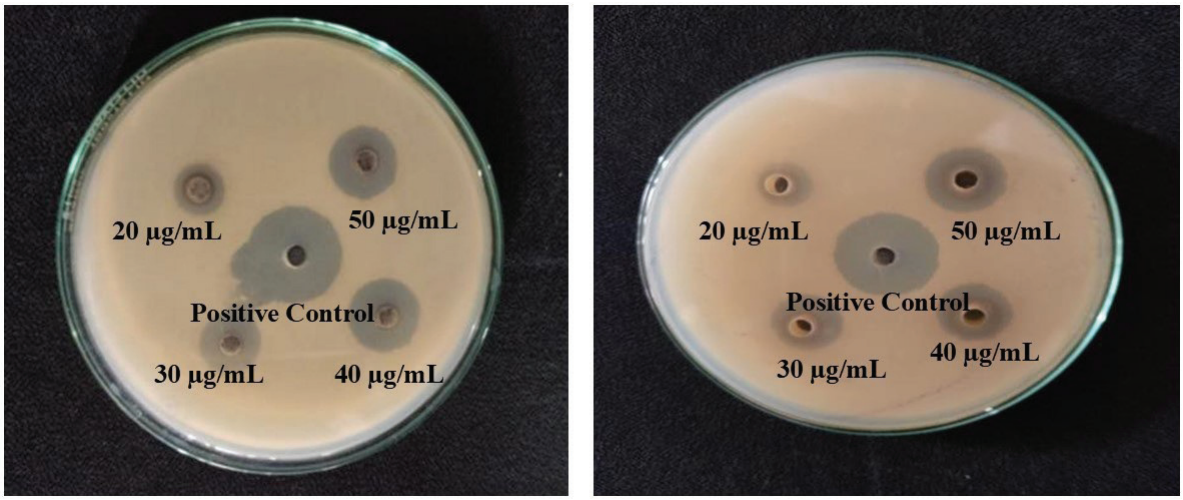

Bacillus cereus *Shigella flexneri*

Figure 9. The agar well-diffusion assay showing the dose-dependent antibacterial activity of AgNPs synthesized using *S. jambos* leaf aqueous extract against *Bacillus cereus* (Gram-positive) and *Shigella flexneri* (Gram-negative). Clear inhibition zones increased with AgNP concentration from 20 µg/mL to 50 µg/mL. Ciprofloxacin (10 µg/mL) was used as a positive control.

Table 1. Inhibitory zones developed for two infective bacterial strains (Gram-positive and Gram-negative) showing dose-dependant antibacterial activity.

Doses (µg/mL)	Inhibitory zone (mm)	
	Bacillus cereus	*Shigella flexneri*
20	5.2 ± 0.70	4.0 ± 0.20
30	7.0 ± 0.54	5.1 ± 0.90
40	8.1 ± 0.31	6.3 ± 0.36
50	10.3 ± 0.62	8.0 ± 0.40
Antibiotic (ciprofloxacin, 10 µg/mL)	13.0 ± 0.20$^{a–c}$	10.0 ± 0.82$^{d–f}$

Notes: $^{a–c}$Significance ($P < 0.05$), compared to 20 µg/mL, 30 µg/mL, and 40 µg/mL against *Bacillus cereus*, respectively.
$^{d–f}$Significance ($P < 0.05$), compared to 20 µg/mL, 30 µg/mL and 40 µg/mL against *Shigella flexneri*, respectively.

growth of zebrafish embryo. The AgNPs were exposed to zebrafish embryo for three different periods. With an upsurge in the doses of AgNPs and exposure intervals, toxicity occurred toward the morphology of zebrafish embryo. At 100 µg/mL, the toxicity was small. AgNPs revealed toxicity at 200 µg/mL and 300 µg/mL toward zebrafish embryo. The notochord of zebrafish appeared bent, with visualized edema of the pericardial, abnormalities of the eyes and craniofacial and yolk sac edema deformations (Figure 10). With increase in the dose of AgNPs, the exterior of fertilized eggs turned rough and the yolk sac was distorted, thus impacting the survival and development of the embryo. No such alteration of morphology was observed in untreated zebrafish larvae.

Discussion

The AgNPs synthesized utilizing the aqueous extracts of *Pedalium murex* (leaf extract), *Piper nigrum, Saraca indica* (leaf extract), and *Capsicum annuum* L. (juice) also manifested dark-brownish coloration (Anandalakshmi *et al.*, 2016; Li *et al.*, 2007; Paulkumar *et al.*, 2014). Our results were in concordance with other investigations. The functional groups (carboxylic and hydroxyl) of secondary metabolites after losing hydrogen ions achieve negative charge and acquire electrostatic form of interaction with silver ions, which efficaciously facilitate the biological reduction of silver ions to zero valent silver ions (Ag0), aiding in the creation of AgNPs (Safa and Koohestani, 2024). The electromagnetic field that stimulates electron oscillation in the conductive band region of AgNPs is the pivotal contributor of SPR (Mollick *et al.*, 2019). AgNPs synthesized using *Moringa oleifera* aqueous leaf extract presented peak at 419 nm, which was very close to our outcome (Asif *et al.*, 2022). *Berberis asiatica* root aqueous extract-designed AgNPs formed peak at 427 nm. Additionally, the SPR of AgNPs is governed by dielectric trait, dimension, morphology, and the elemental composition of fabricated AgNPs (Dangi *et al.*, 2020). The leaf aqueous extract of *Cucumis prophetarum* and silver nitrate-blended AgNPs had a defined peak at 420 nm (Hemlata *et al.*, 2020). Also, an aqueous leaf extract of *Morinda lucida*-fabricated AgNPs showed peak at 420 nm. The phytometabolites (proteins, steroids, tannins, phenols, saponins, and flavonoids) aid in the bio-based reduction of silver ions to AgNPs (Labulo *et al.*, 2022).

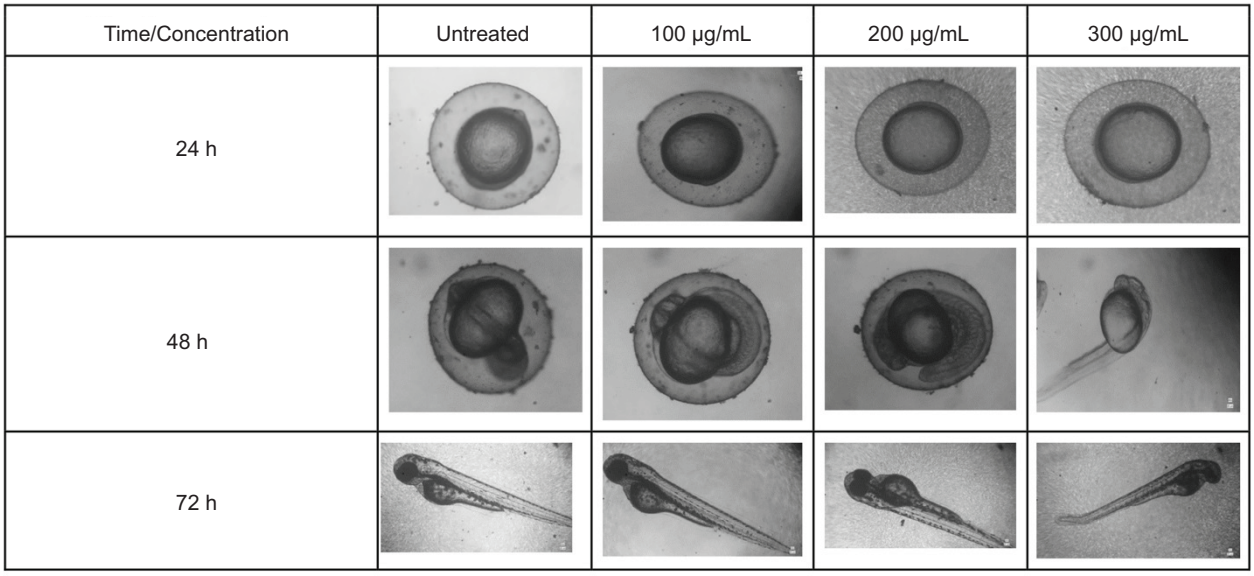

Figure 10. Toxicity effects of AgNPs synthesized using *S. jambos* leaf aqueous extract on zebrafish embryo at 24, 48, and 72 h post-exposure. Increased concentrations (100, 200, and 300 µg/mL) induced morphological abnormalities, including bent notochord, pericardial edema, craniofacial deformities, eye abnormalities, and yolk sac edema. Control embryos showed normal development with no morphological alterations.

The functional group attributed to M-O (metal-oxygen) bonding, specifically Ag-O bonding, appeared at 583 cm^{-1} (Patra and Baek, 2017). The C-C stretching vibrational peak that appeared at 1,402 cm^{-1} dictated aromatic structural compound's existence. Peak that emerged at 1,112 cm^{-1} signified amine group's C-N vibrational stretching. An intensive peak formed at 618 cm^{-1} revealed alkyl group's C-Cl vibrational stretching. Glycosides, phenolic acids, saponins, tannins, and flavonoids aided in the phyto-based formation of AgNPs (Dobrucka *et al.*, 2019). Usually, the interaction of silver ions with the plant's bioactive molecules encourages the formation of zero valent silver ions from silver ions via reduction. Precisely, from the enolic group of phytophenolic compound, electron is released through the breaking of hydroxyl bond. This electron is utilized in the genesis of AgNPs. The broader peak (OH group peak) that appeared in the spectra of FTIR, justified its involvement in the phyto-designed development of AgNPs (Sukweenadhi *et al.*, 2021).

The AgNPs designed by applying the aqueous extract of *Moringa oleifera* and *Phlomis* leaf provided XRD diffraction spectra similar to our result (Haris and Ahmad, 2024). Additional peak presented the participation of phyto-organic molecules in the fabrication of AgNPs (Karuppiah and Rajmohan, 2013). Even the *Momordica cymbalaria* (fruit extract)- and *Cydonia oblong* (seed extract)-utilized AgNPs also manifested similar sort of diffraction pattern through XRD study (Zia *et al.*, 2016). Higher surface area and greater energy of the fabricated AgNPs were attributable to their aggregation facilitated by physical force (Vander Waal's force). The AgNPs using *Salvia spinosa* (seed extract) and *Strychnos potatorum* Linn F (leaf extract) also demonstrated spheroidal shape (Kagithoju et al., 2015). Spheroidal AgNPs with 45-nm dimension were formed when Flax seed extract was used for procurement (Alzubaidi *et al.*, 2023). The AgNPs designed by applying the aqueous leaf extract of *Perilla* also had spheroidal shape with less than 50-nm dimension (Sharma *et al.*, 2024). Even, the outcome was in exact parallelism to the previous data. AgNPs synthesized using the extract of *Camellia sinesis* var. (Chinese green tea) had spheroidal shape coated with phytomolecules with a mean dimension of 35.76 nm (Al-Otibi *et al.*, 2023). Similarly, the AgNPs acquired by applying the *Ctenolepis garcinia* L. aqueous leaf extract also had spheroidal shape, with dimensional range of 10–25 nm (Narayanan *et al.*, 2021). Phytochemicals could also act as capping agents for the synthesis of nanoparticles (Siddique *et al.*, 2024).

The AgNPs created from the water fruit extract of *Prosopis farcta* showed dose-mannered increment in the percentage of DPPH inhibition. At 0.2 mg/mL of AgNPs, the DPPH inhibition was 43%, and at 1 mg/mL of AgNPs, the inhibition was 63%, with 0.70 mg/mL as IC_{50} value. Nanosilver had superior anti-radical function, compared to the fruit extract. AgNPs synthesized using the aqueous leaf extract of *Erythrina suberosa* displayed marvellous anti-radical potency with 30.04 µg/mL as IC_{50} value (Mohanta *et al.*, 2017). Similarly, AgNPs fabricated

by utilizing the aqueous leaf extract of *Brassica oleracea* provided dose-responsive (50–200 µg/mL) form of anti-radical activity through DPPH assay, with an IC_{50} of 50.37 µg/mL. The biological potential of extracts of *Kadsua coccinea* leaves evaluated by *in vitro* antioxidant assay showed promising DPPH scavenging activity (Shi *et al.*, 2022). The phytoingredient's phenolic and hydroxyl (OH) function groups layer on the AgNPs would have donated the electron/hydrogen and aided in the anti-radical function of the nanoparticles (Ansar *et al.*, 2020). The aqueous root extract of *Helicteres isora*-applied phyto-formulated AgNPs also showed dose-basis (10–100 µg/mL) anti-radical efficacy with 90% DPPH radical inhibition (Bhakya *et al.*, 2016). In accordance with these reports, the DPPH inhibition would be due to a synergistic action of AgNPs and the phenolic content present on the surface of nanoparticles, both of which portray anti-radical effect by donating electrons/hydrogen.

Amid free radicals, NO is a highly diffusible bioregulatory form and has indispensable functions in the human body, such as anticancer, relaxation of smooth muscles, neurological messenger, hindering platelet's aggregation, microbicidal, and controlling cellular-influenced toxicity (Andrabi *et al.*, 2023). Chronic generation of NO upsurges the issue of carcinoma, inflammation, diabetes mellitus, ulcerative colitis, Alzheimer's disease, heart diseases, and autoimmune conditions (rheumatoid arthritis and multiple sclerosis) (Roy *et al.,* 2013). Phytophenolics also confer NO scavenging ability. As appeared in our investigations, AgNPs wrapped with the fruit extract of *Piper longum* delivered increased percentage inhibition of NO ions in a dose-dependent manner (Shi *et al.*, 2022). At a maximum dose of 500 µg/mL, the NO percentage inhibition shown by AgNPs was 70%, which was greater, compared to fruit extract.

Usually, the lower stabilized NO ion acquires electron from AgNPs and develops formazan on blending with Griess reagent and monitored spectrophotometrically (Reddy *et al.*, 2014). AgNPs designed by adopting the aqueous leaf extract of *Decaschistia crotonifolia* showed 64.98% of NO inhibition, whereas 52.64% of NO inhibition was shown by *Decaschistia crotonifolia* leaf extract at 100-µg/mL dose. Both samples projected dose-based NO scavenging function (Palithya *et al.,* 2021). Similarly, NO scavenging efficacy of the AgNPs designed from the aqueous pod extract of *Pisum sativum* L. was entirely dose-related when screened from 10 µg/mL to 50 µg/mL. Phytophenolics, in addition to nanoparticle's stabilization, also render antioxidative function toward free radicals (Alarjani *et al.*, 2022).

Our antibacterial results confirmed the previously reported outcomes. Nanosilver acquired through the application of leaf extract of *Plumeria alba* (frangipani) when screened offered excellent antibacterial performance toward both classes of bacteria (Gram +ve and Gram -ve), such as *Bacillus subtilis*, *Enterococcus faecalis*, *Streptococcus pneumonia*, and *Enterobacter aerogenes*, in a dose-dependent manner at a concentration of 25–100 µg/mL, with pronounced inhibitory zone at a higher dose (100 µg/mL) (Rudrappa *et al.*, 2022). Bharadwaj *et al.* (2021) showed that the spheroidal-shaped AgNPs using the fruit extract of *Diospyros malabarica* appeared to be bactericidal toward *Staphylococcus aureus* and *Escherichia coli* at two varying doses (500 µg/mL and 1,000 µg/mL).

Numerous mechanistic ways have been suggested for the bactericidal functionalities of AgNPs. The amino, phosphate, and carboxylic groups are attributed to the negative charge of bacterial cellular membrane (Mortazavi-Derazkola *et al.,* 2021). The positive charge of AgNPs and the bacterial cell negative charge create electrostatic force between the two components enduring efficacious binding. AgNPs trigger the genesis of pit on bacterial cellular surface, which aid in the feasible penetrability of silver ions (Firdhouse and Lalitha, 2016). AgNPs strongly bind to the S-H (thiol) group of the enzymes containing sulphur and develop sulphur-silver (S-Ag) bond, thereby hindering the transport of crucial ions by those enzymes. The reactive oxygen species (ROS) molecules encourage the hydrogen bonding interruption between the anti-parallel polynucleotide strands of DNA and facilitate its denaturation by intercalating nitrogenous bases (purine/pyrimidine) (Yassin *et al.*, 2022).

Macromolecular component (protein/reducing sugar) leakage from the bacterial cell was intended to damage cellular membrane permeability, thus leading to bacterial lysis (Sharma *et al.*, 2009). The adherence of AgNPs to bacterial cell wall renders denaturation of proteins, loss of proton motive force through the precursor protein built-up eventually enhancing cellular killing (Jemilugba *et al.*, 2019). Even lipids and lipopolysaccharides (LPS) of bacterial cellular membranes were also tremendously damaged by AgNPs. The exterior charge, surface nature, and concentration of nanoparticles have marvellous impact on bactericidal activity (Abdelsattar *et al.,* 2022). Smaller dimension of AgNPs enriches its bactericidal function by offering easy penetration and huge-surface space for better interaction, facilitating the release of silver (Ag^0) ions (Kathiravan *et al.,* 2015). Superoxide anion, a form of ROS, stimulates oxidative-type of stress within the bacterial cells, promoting the interruption of electron transport chain (ETC), mutation, and damage to genome content (Nishanthi et al., 2019). A study done by Zeng *et al*. 2020, explained anti-nociceptive and bioactive phytoingredients present in the extracts of *Typha angustifolia* L that could offer therapeutic outcome. Similarly,

the plant extracts of *S. jambos* also showed therapeutic potential, and the phenolic ingredient layered on AgNPs also contributed to efficacious bactericidal potential (Esmaile *et al.*, 2020). Similarly, the present study also showed antibacterial effect against both organisms due to the positive charge present on the surface of the nanoparticles. This was further enhanced by the phenolic content present on the surface of plant extract.

A study done by Xia *et al.* (2016) reported that at 10 mg/L of AgNPs dose, the surviving embryo projected malformations and degeneration of body after 48 h. The nano spheroidal silver particles synthesized using the green tea extract also showed similar forms of morphological alterations as reported in our study, thus demonstrating the toxicity of nanoparticles (Girigoswami *et al.,* 2024). Similarly, AgNPs synthesized by utilizing seed extract of *Syzygium aromaticum* showed moderate level of toxicity toward the growth and formation of zebrafish embryo at a dose of 50 µg/mL. Greater toxicity occurred at 75 µg/mL and 100 µg/mL of the applied AgNPs on the embryo of zebrafish (Dhanislas *et al.*, 2023).

Multifunctional nanoparticles portray significant applications in various fields. A study done by Jabbar *et al.* (2023) showed the ability to detect chemical ions using plant extract functionalized AgNPs as well as antimicrobial activity. Similarly, the AgNPs developed using extracts of *S. jambos* could provide multifunctional capability as evidenced through antioxidant and antibacterial properties. The safe use of nanoparticles in multifarious applications is studied. Regulations demand thorough physicochemical characterization, *in vitro* and *in vivo* toxicity evaluations, and other biochemical interactions prior to being implemented on humans (Wang and Tang, 2021).

Conclusions

In the executed study, a cost-effective and environment-friendly phyto-based methodology was followed to procure AgNPs from the aqueous leaf extract of *S. jambos*. The transformation of Ag^0 to AgNPs was considered by the formation of dark-brownish color by mixing the leaf aqueous extract of *S. jambos* with silver nitrate solution. The physiochemical and microscopic characterization was done for the created AgNPs. A peak at 420 nm justified the formation of AgNPs via UV-vis spectroscopy. FTIR spectra showed the role of glycosides, phenolic acids, saponins, tannins, and flavonoids in the reduction, stabilization, and capping of nanoparticles. XRD demonstrated crystallinity and grain size (17.8 nm) of the designed nanoparticles. In SEM and TEM micrographic images, the fabricated nanoparticles conveyed spheroidal morphology with agglomeration and had an average dimension of 18.9 nm. The EDX spectra revealed silver, oxygen, and carbon. Through DPPH and NO assays, it was conveyed that the fabricated AgNPs quelled both free radicals in a dose-dependent manner. AgNPs showed effective inhibitory performance toward the screened *Bacillus cereus* and *Shigella flexneri*. Moreover, AgNPs were toxic toward zebrafish embryo by creating phenotypic deformities and also impacting its growth. This zebrafish embryo toxicity study aids in screening the beneficial concentration of AgNPs, so that it could be practised in the biomedical field for versatile applications. Overall, more experimental trials have to be conducted on various bioactivities of AgNPs to enhance their applications. In-depth molecular mechanistic studies must be performed to acquire the detailed mode of AgNPs functioning for therapeutic usage.

Acknowledgements

The author is thankful to the Deanship of Graduate Studies and Scientific Research at University of Bisha for supporting this work through the Fast-Track Research Support Program.

Data Availability Statement

All data generated and analyzed in this study are included in this article.

Author Contributions

Mosleh Mohammad Abomughaid: conceptualization, methodology, validation, formal analysis, investigation, data curation, writing—original draft, review and editing, and project administration.

Conflicts of Interest

The author declared no conflict of interest.

Acknowledgements

The author is thankful to the Deanship of Graduate Studies and Scientific Research at University of Bisha for supporting this work through the Fast-Track Research Support Program.

Funding

None.

References

Abdallah, S.A, Hakim, T.A., Rezk, N., Farouk, W.M., Hassan, Y.Y., Gouda, S.M. and El-Shibiny, A. 2022. Green synthesis of silver nanoparticles using Ocimum basilicum L. and Hibiscus sabdariffa L. extracts and their antibacterial activity in combination with phage ZCSE6 and sensing properties. Journal of Inorganic and Organometallic Polymers and Materials 32(6): 1951–1965. https://doi.org/10.1007/s10904-022-02234-y

Alarjani, K.M., Huessien, D., Rasheed, R.A. and Kalaiyarasi, M. 2022. Green synthesis of silver nanoparticles by Pisum sativum L. (pea) pod against multidrug resistant foodborne pathogens. Journal of King Saud University – Science 34(3): 101897. https://doi.org/10.1016/j.jksus.2022.101897

Alex, A.M., Subburaman, S., Chauhan, S., Ahuja, V., Abdi, G. and Tarighat, M.A. 2024. Green synthesis of silver nanoparticle prepared with Ocimum species and assessment of anticancer potential. Scientific Reports 14(1): 11707. https://doi.org/10.1038/s41598-024-61946-y

Al-Otibi, F.O., Yassin, M.T., Al-Askar, A.A. and Maniah, K. 2023. Green biofabrication of silver nanoparticles of potential synergistic activity with antibacterial and antifungal agents against some nosocomial pathogens. Microorganisms 11(4): 945. https://doi.org/10.3390/microorganisms11040945

Alzubaidi, A.K., Al-Kaabi, W.J., Ali, A.A., Albukhaty, S., Al-Karagoly, H., Sulaiman, G.M., Asiri, M. and Khane, Y. 2023. Green synthesis and characterization of silver nanoparticles using flaxseed extract and evaluation of their antibacterial and antioxidant activities. Applied Sciences 13(4): 2182. https://doi.org/10.3390/app13042182

Anandalakshmi, K., Venugobal, J. and Ramasamy, V. 2016. Characterization of silver nanoparticles by green synthesis method using Pedalium murex leaf extract and their antibacterial activity. Applied Nanoscience 6: 399–408. https://doi.org/10.1007/s13204-015-0449-z

Anbumani, D., Dhandapani, K.V., Manoharan, J., Babujanarthanam, R., Bashir, AKH, Muthusamy, K., Alfarhan, A. and Kanimozhi, K. 2022. Green synthesis and antimicrobial efficacy of titanium dioxide nanoparticles using Luffa acutangula leaf extract. Journal of King Saud University – Science 34(3): 101896. https://doi.org/10.1016/j.jksus.2022.101896

Andrabi, S.M., Sharma, N.S., Karan, A., Shahriar, S.S.M., Cordon, B., Ma, B. and Xie, J. 2023. Nitric oxide: physiological functions, delivery, and biomedical applications. Advanced Science 10(30): 2303259. https://doi.org/10.1002/advs.202303259

Ansar, S., Tabassum, H., Aladwan, Norah S.M., Ali, M.N., Almaarik, B., AlMahrouqi, S., Abudawood, M., Banu, N. and Alsubki, R. 2020. Eco-friendly silver nanoparticles synthesis by Brassica oleracea and its antibacterial, anticancer and antioxidant properties. Scientific Reports 10(1): 18564. https://doi.org/10.1038/s41598-020-74371-8

Arshad, F., Naikoo, G.A., Hassan, I.U., Chava, S.R., El-Tanani, M., Aljabali, A.A. and Tambuwala, M.M. 2024. Bioinspired and green synthesis of silver nanoparticles for medical applications: a green perspective. Applied Biochemistry and Biotechnology 196(6): 3636–3669. https://doi.org/10.1007/s12010-023-04719-z

Asif, M., Yasmin, R., Asif, R., Ambreen, A., Mustafa, M. and Umbreen, S. 2022. Green synthesis of silver nanoparticles (AgNPs), structural characterization, and their antibacterial potential. Dose-Response 20(2):15593258221088709. https://doi.org/10.1177/15593258221088709

Avila-Peña, D., Peña, N., Quintero, L. and Suárez-Roca, H. 2007. Antinociceptive activity of Syzygium jambos leaves extract on rats. Journal of Ethnopharmacology 112(2): 380–385. https://doi.org/10.1016/j.jep.2007.03.027

Baghizadeh, A., Ranjbar, S., Gupta, V.K., Asif, M., Pourseyedi, S., Karimi, M.J. and Mohammadinejad, R. 2015. Green synthesis of silver nanoparticles using seed extract of Calendula officinalis in liquid phase. Journal of Molecular Liquids 207: 159–163. https://doi.org/10.1016/j.molliq.2015.03.029

Balkrishna, A., Kumar, A., Arya, V., Rohela, A., Verma, R., Nepovimova, E., Krejcar, O., Kumar, D., Thakur, N. and Kuca, K. 2021. Phytoantioxidant functionalized nanoparticles: a green approach to combat nanoparticle-induced oxidative stress. Oxidative Medicine and Cellular Longevity 2021(1): 3155962. https://doi.org/10.1155/2021/3155962

Baskaran, R., Chen, Yi-Ju, Chang, Ching-Fang, Kuo, Hsin-Ning, Liang, Chih-Hung, Abomughaid, M.M., Senthil Kumar, K.J. and Lin, Wan-Teng. 2025. Potato protein hydrolysate (PPH902) exerts anti-lipogenesis and lipolysis-promoting effect by inhibiting adipogenesis in 3T3-L1 adipocytes. 3 Biotech 15(4): 83. https://doi.org/10.1007/s13205-025-04238-0

Bhakya, S, Muthukrishnan, S., Sukumaran, M. and Muthukumar, M. 2016. Biogenic synthesis of silver nanoparticles and their antioxidant and antibacterial activity. Applied Nanoscience 6: 755–766. https://doi.org/10.1007/s13204-015-0473-z

Bharadwaj, K.K., Rabha, B., Pati, S., Choudhury, B.K., Sarkar, T., Gogoi, S.K., Kakati, N., Baishya, D., Abdul Kari, Z. and Edinur, H.T. 2021. Green synthesis of silver nanoparticles using Diospyros malabarica fruit extract and assessments of their antimicrobial, anticancer and catalytic reduction of 4-nitrophenol (4-NP). Nanomaterials 11(8): 1999. https://doi.org/10.3390/nano11081999

Bordiwala, R.V. 2023. Green synthesis and applications of metal nanoparticles – a review article. Results in Chemistry 5: 100832. https://doi.org/10.1016/j.rechem.2023.100832

Borquaye, L.S., Laryea, M.K., Gasu, E.N., Boateng, M.A., Baffour, P.K., Kyeremateng, A. and Doh, G. 2020. Anti-inflammatory and antioxidant activities of extracts of Reissantia indica, Cissus cornifolia and Grosseria vignei. Cogent Biology 6(1): 1785755. https://doi.org/10.1080/23312025.2020.1785755

Chaudhari, R.K., Shah, P.A. and Shrivastav, P.S. 2023. Green synthesis of silver nanoparticles using Adhatoda vasica leaf extract and its application in photocatalytic degradation of dyes. Discover Nano 18(1): 135. https://doi.org/10.1186/s11671-023-03914-5

Chaudhary, P., Janmeda, P., Docea, A.O., Yeskaliyeva, B., Razis, A.A.F., Modu, B., Calina, D. and Sharifi-Rad, J. 2023. Oxidative stress, free radicals and antioxidants: potential crosstalk in the pathophysiology of human diseases. Frontiers in Chemistry 11: 1158198. https://doi.org/10.3389/fchem.2023.1158198

Chinnaraj, S., Palani, V., Maluventhen, V., Chandrababu, R., Soundarapandian, K., Kaliannan, D., Rathinasamy, B., Liu, W-C.,

Balasubramanian, B. and Arumugam, M. 2023. Silver nanoparticle production mediated by Goniothalamus wightii extract: characterization and their potential biological applications. Particulate Science and Technology 41(4): 517–531. https://doi.org/10.1080/02726351.2022.2123752

Dakshayani, S.S., Marulasiddeshwara, M.B., Kumar, S., Golla, R., Devaraja, S.R.H.K. and Hosamani, R. 2019. Antimicrobial, anticoagulant and antiplatelet activities of green synthesized silver nanoparticles using Selaginella (Sanjeevini) plant extract. International Journal of Biological Macromolecules 131: 787–797. https://doi.org/10.1016/j.ijbiomac.2019.01.222

Dangi, S., Gupta, A., Gupta, D.K., Singh, S. and Parajuli, N. 2020. Green synthesis of silver nanoparticles using aqueous root extract of Berberis asiatica and evaluation of their antibacterial activity. Chemical Data Collections 28: 100411. https://doi.org/10.1016/j.cdc.2020.100411

Dhandapani, K.V., Anbumani, D., Gandhi, A.D., Annamalai, P., Muthuvenkatachalam, B.S., Kavitha, P. and Ranganathan, B. 2020. Green route for the synthesis of zinc oxide nanoparticles from Melia azedarach leaf extract and evaluation of their antioxidant and antibacterial activities. Biocatalysis and Agricultural Biotechnology 24: 101517. https://doi.org/10.1016/j.bcab.2020.101517

Dhanislas, M., Sampath, S., Shamya, M., Joseph, J., Yasasve, M., Ahmed, M.Z., Alqahtani, A.S., Kazmi, S., Asaithambi, P. and Suresh, A. 2023. Green synthesis of biofabricated silver nanoparticles from Syzygium aromaticum seeds: spectral characterization and evaluation of its anti-mycobacterial activity, cytotoxicity assessment on zebrafish embryo and Artemia salina. Materials Technology 38(1): 2269358. https://doi.org/10.1080/10667857.2023.2269358

Dobrucka, R., Szymanski, M. and Przekop, R. 2019. The study of toxicity effects of biosynthesized silver nanoparticles using Veronica officinalis extract. International Journal of Environmental Science and Technology 16(12): 8517–8526. https://doi.org/10.1007/s13762-019-02441-0

Dutta, P.P., Bordoloi, M., Gogoi, K., Roy, S., Narzary, B., Bhattacharyya, D.R., Mohapatra, P.K. and Mazumder, B. 2017. Antimalarial silver and gold nanoparticles: green synthesis, characterization and in vitro study. Biomedicine & Pharmacotherapy 91: 567–580. https://doi.org/10.1016/j.biopha.2017.04.032

Esmaile, F., Koohestani, H. and Abdollah-Pour, H. 2020. Characterization and antibacterial activity of silver nanoparticles green synthesized using Ziziphora clinopodioides extract. Environmental Nanotechnology, Monitoring & Management 14: 100303. https://doi.org/10.1016/j.enmm.2020.100303

Firdhouse, M.J. and Lalitha, P. 2016. Biogenic silver nanoparticles – synthesis, characterization and its potential against cancer inducing bacteria. Journal of Molecular Liquids 222: 1041–1050. https://doi.org/10.1016/j.molliq.2016.07.141

Ganeshkumar, M., Sastry, T.P.M., Kumar, S., Dinesh, M.G., Kannappan, S. and Suguna, L. 2012. Sun light mediated synthesis of gold nanoparticles as carrier for 6-mercaptopurine: preparation, characterization and toxicity studies in zebrafish embryo model. Materials Research Bulletin 47(9): 2113–2119. https://doi.org/10.1016/j.materresbull.2012.06.015

Ghojavand, S., Madani, M. and Karimi, J. 2020. Green synthesis, characterization and antifungal activity of silver nanoparticles using stems and flowers of felty germander. Journal of Inorganic and Organometallic Polymers and Materials 30: 2987–2997. https://doi.org/10.1007/s10904-020-01449-1

Girigoswami, A., Meenakshi, S., Deepika, B., Harini, K., Gowtham, P., Pallavi, P. and Girigoswami, K. 2024. Beneficial effects of bioinspired silver nanoparticles on zebrafish embryos including a gene expression study. ADMET and DMPK 12(1): 177–192. https://doi.org/10.5599/admet.2102

Han, H.S., Koo, S.Y. and Choi, K.Y. 2022. Emerging nanoformulation strategies for phytocompounds and applications from drug delivery to phototherapy to imaging. Bioactive Materials 14: 182–205. https://doi.org/10.1016/j.bioactmat.2021.11.027

Haris, Z. and Ahmad, I. 2024. Green synthesis of silver nanoparticles using Moringa oleifera and its efficacy against gram-negative bacteria targeting quorum sensing and biofilms. Journal of Umm Al-Qura University for Applied Sciences 10(1): 156–167. https://doi.org/10.1007/s43994-023-00089-8

Hemlata, P.R.M., Singh, A.P. and Tejavath, K.K. 2020. Biosynthesis of silver nanoparticles using Cucumis prophetarum aqueous leaf extract and their antibacterial and antiproliferative activity against cancer cell lines. ACS Omega 5(10): 5520–5528. https://doi.org/10.1021/acsomega.0c00155

Hu, D., Gao, T., Kong, X., Jinhong F.N.M., Meng, L., Duan, X., Hu, C.Y., Chen, W. and Feng, Z. 2022. Ginger (*Zingiber officinale*) extract mediated green synthesis of silver nanoparticles and evaluation of their antioxidant activity and potential catalytic reduction activities with Direct Blue 15 or Direct Orange 26. Plos One 17(8): e0271408. https://doi.org/10.1371/journal.pone.0271408

Huh, A.J. and Kwon, Y.J. 2011. "Nanoantibiotics": a new paradigm for treating infectious diseases using nanomaterials in the antibiotics resistant era. Journal of Controlled Release 156(2): 128–145. https://doi.org/10.1016/j.jconrel.2011.07.002

Jabbar, A., Abbas, A., Assad, N., Naeem-ul-Hassan, M., Alhazmi, H.A., Najmi, A., Zoghebi, K., Al Bratty, M., Hanbashi, A. and Amin, H.M.A. 2023. A highly selective Hg2+ colorimetric sensor and antimicrobial agent based on green synthesized silver nanoparticles using Equisetum diffusum extract. RSC Advances 13(41): 28666–28675. https://doi.org/10.1039/D3RA05070J

Jain, N., Jain, P., Rajput, D. and Patil, U.K. 2021. Green synthesized plant-based silver nanoparticles: therapeutic prospective for anticancer and antiviral activity. Micro and Nano Systems Letters 9(1): 5. https://doi.org/10.1186/s40486-021-00131-6

Jamkhande, P.G., Ghule, N.W., Bamer, A.H. and Kalaskar, M.G. 2019. Metal nanoparticles synthesis: an overview on methods of preparation, advantages and disadvantages, and applications. Journal of Drug Delivery Science and Technology 53: 101174. https://doi.org/10.1016/j.jddst.2019.101174

Jeevanandam, J., Krishnan, S., Hii, Y.S., Pan, S., Chan, Y.S., Acquah, C., Danquah, M.K. and Rodrigues, J. 2022. Synthesis approach-dependent antiviral properties of silver nanoparticles and nanocomposites. Journal of Nanostructure in Chemistry 12(5): 1–23. https://doi.org/10.1007/s40097-021-00465-y

Jemilugba, O.T., Parani, S., Mavumengwana, V. and Oluwafemi, O.S. 2019. Green synthesis of silver nanoparticles using Combretum

erythrophyllum leaves and its antibacterial activities. Colloid and Interface Science Communications 31: 100191. https://doi.org/10.1016/j.colcom.2019.100191

Kagithoju, S., Godishala, V. and Nanna, R.S. 2015. Eco-friendly and green synthesis of silver nanoparticles using leaf extract of Strychnos potatorum Linn. F. and their bactericidal activities. 3 Biotech 5: 709–714. https://doi.org/10.1007/s13205-014-0272-3

Kajani, A.A., Bordbar, A-K., Esfahani, S.H.Z., Khosropour, A.R. and Razmjou, A. 2014. Green synthesis of anisotropic silver nanoparticles with potent anticancer activity using Taxus baccata extract. RSC Advances 4(106): 61394–61403. https://doi.org/10.1039/C4RA08758E

Karuppiah, M. and Rajmohan, R. 2013. Green synthesis of silver nanoparticles using Ixora coccinea leaves extract. Materials Letters 97:141–143. https://doi.org/10.1016/j.matlet.2013.01.087

Kathiravan, V., Ravi, S., Ashokkumar, S., Velmurugan, S., Elumalai, K. and Khatiwada, C.P. 2015. Green synthesis of silver nanoparticles using Croton sparsiflorus morong leaf extract and their antibacterial and antifungal activities. Spectrochimica Acta Part A: Molecular and Biomolecular Spectroscopy 139: 200–205. https://doi.org/10.1016/j.saa.2014.12.022

Keshari, A., Srivastava, R., Yadav, S., Nath, G. and Gond, S. 2020. Synergistic activity of green silver nanoparticles with antibiotics. Nanomedicine Research Journal 5(1): 44–54.

Khan, H.A., Ghufran, M., Shams, S., Jamal, A., Khan, A., Abdullah, A., Zuhier, A. and Khan, M.I. 2023. Green synthesis of silver nanoparticles from plant Fagonia cretica and evaluating its anti-diabetic activity through indepth in-vitro and in-vivo analysis. Frontiers in Pharmacology 14: 1194809. https://doi.org/10.3389/fphar.2023.1194809

Kora, A.J. and Rastogi, L. 2018. Green synthesis of palladium nanoparticles using gum ghatti (Anogeissus latifolia) and its application as an antioxidant and catalyst. Arabian Journal of Chemistry 11(7): 1097–1106. https://doi.org/10.1016/j.arabjc.2015.06.024

Labulo, A.H., David, O.A. and Terna, A.D. 2022. Green synthesis and characterization of silver nanoparticles using Morinda lucida leaf extract and evaluation of its antioxidant and antimicrobial activity. Chemical Papers 76(12): 7313–7325. https://doi.org/10.1007/s11696-022-02392-w

Li, S., Shen, Y., Xie, A., Yu, X., Qiu, L., Zhang, L. and Zhang, Q. 2007. Green synthesis of silver nanoparticles using Capsicum annuum L. extract. Green Chemistry 9(8): 852–858. https://doi.org/10.1039/b615357g

Mahiuddin, Md., Saha, P. and Ochiai, B. 2020. Green synthesis and catalytic activity of silver nanoparticles based on Piper chaba stem extracts. Nanomaterials 10(9): 1777. https://doi.org/10.3390/nano10091777

Mahmoodi, E., Hassan, K., Abolghasem A. and Bordbar, A-K. 2018. Green synthesis of silver nanoparticles using flower extract of Malva sylvestris and investigation of their antibacterial activity. IET Nanobiotechnology 12(4): 412–416. https://doi.org/10.1049/iet-nbt.2017.0166

Masum, Md., Mahidul, I., Siddiqa, M.M., Ali, K.A., Zhang, Y., Abdallah, Y., Ibrahim, E., Qiu, W., Yan, C. and Li, B. 2019. Biogenic synthesis of silver nanoparticles using Phyllanthus emblica fruit extract and its inhibitory action against the pathogen Acidovorax oryzae strain RS-2 of rice bacterial brown stripe. Frontiers in Microbiology 10: 820. https://doi.org/10.3389/fmicb.2019.00820

Mohanta, Y.K., Panda, S.K., Jayabalan, R., Sharma, N., Bastia, A.K. and Mohanta, T.K. 2017. Antimicrobial, antioxidant and cytotoxic activity of silver nanoparticles synthesized by leaf extract of Erythrina suberosa (Roxb.). Frontiers in Molecular Biosciences 4: 14. https://doi.org/10.3389/fmolb.2017.00014

Mollick, M.M.R., Rana, D., Dash, S.K., Chattopadhyay, S., Bhowmick, B., Maity, D., Mondal, D., Pattanayak, S., Roy, S. and Chakraborty, M. 2019. Studies on green synthesized silver nanoparticles using Abelmoschus esculentus (L.) pulp extract having anticancer (*in vitro*) and antimicrobial applications. Arabian Journal of Chemistry 12(8): 2572–2584. https://doi.org/10.1016/j.arabjc.2015.04.033

Mortazavi-Derazkola, S., Yousefinia, A., Naghizadeh, A., Lashkari, S. and Hosseinzadeh, M. 2021. Green synthesis and characterization of silver nanoparticles using Elaeagnus angustifolia bark extract and study of its antibacterial effect. Journal of Polymers and the Environment 29(March): 3539–3547. https://doi.org/10.1007/s10924-021-02122-5

Narayanan, M., Divya, S., Natarajan, D., Senthil-Nathan, S., Kandasamy, S., Chinnathambi, A., Alahmadi, T.A. and Pugazhendhi, A. 2021. Green synthesis of silver nanoparticles from aqueous extract of Ctenolepis garcini L. and assess their possible biological applications. Process Biochemistry 107: 91–99. https://doi.org/10.1016/j.procbio.2021.05.008

Nishanthi, R., Malathi, S. and Palani, P. 2019. Green synthesis and characterization of bioinspired silver, gold and platinum nanoparticles and evaluation of their synergistic antibacterial activity after combining with different classes of antibiotics. Materials Science and Engineering: C 96: 693–707. https://doi.org/10.1016/j.msec.2018.11.050

Noppradit, B., Chaiyosburana, S., Khupsathianwong, N., Aemaeg, T., Weena, W., Yupa and Phengdaam, A. 2023. Green synthesis of silver nanoparticles using Saccharum officinarum leaf extract for antiviral paint. Green Processing and Synthesis 12(1): 20230172. https://doi.org/10.1515/gps-2023-0172

Ochieng, M.A., Bakrim, W.B., Bitchagno, G.T.M., Mahmoud, M.F. and Sobeh, M. 2022. Syzygium jambos L. Alston: an insight into its phytochemistry, traditional uses, and pharmacological properties. Frontiers in Pharmacology 13: 786712. https://doi.org/10.3389/fphar.2022.786712

Palithya, S., Gaddam, S.A., Kotakadi, V.S., Penchalaneni, J. and Challagundla, V.N. 2021. Biosynthesis of silver nanoparticles using leaf extract of Decaschistia crotonifolia and its antibacterial, antioxidant, and catalytic applications. Green Chemistry Letters and Reviews 14(1): 137–152. https://doi.org/10.1080/17518253.2021.1876172

Pandey, S., Mewada, A., Thakur, M., Shinde, S., Shah, R., Oza, G. and Sharon, M. 2013. Rapid biosynthesis of silver nanoparticles by exploiting the reducing potential of Trapa bispinosa peel extract. Journal of Nanoscience 2013(1): 516357. https://doi.org/10.1155/2013/516357

Patel, J., Kumar, G.S., Roy, H., Maddiboyina, B., Leporatti, S. and Bohara, R.A. 2024. From nature to nanomedicine: bioengineered metallic nanoparticles bridge the gap for medical applications. Discover Nano 19(1): 1–24. https://doi.org/10.1186/s11671-024-04021-9

Patra, J.K. and Baek, K-H. 2017. Antibacterial activity and synergistic antibacterial potential of biosynthesized silver nanoparticles against foodborne pathogenic bacteria along with its anticandidal and antioxidant effects. Frontiers in Microbiology 8: 167. https://doi.org/10.3389/fmicb.2017.00167

Paulkumar, K, Gnanajobitha, G., Vanaja, M., Rajeshkumar, S., Malarkodi, C., Pandian, K. and Annadurai, G. 2014. Piper nigrum leaf and stem assisted green synthesis of silver nanoparticles and evaluation of its antibacterial activity against agricultural plant pathogens. Scientific World Journal 2014(1): 829894. https://doi.org/10.1155/2014/829894

Priya, L.B., Balasubramanian, B., Shanmugaraj, B., Subbiah, S., Hu, R-M., Huang, C-Y. and Baskaran, R. 2022. Therapeutic potential of the medicinal plant Tinospora cordifolia – minireview. Phyton (0031–9457) 91(6): 1129–1140. https://doi.org/10.32604/phyton.2022.017707

Priya, L.B, Baskaran, R. and Vijaya P.V. 2017. Phytonanoconjugates in oral medicine. In Ecaterina, A., Alexandru, M.G. (eds.): Nanostructures for Oral Medicine. Elsevier, Amsterdam, the Netherlands, pp. 639–668. https://doi.org/10.1016/B978-0-323-47720-8.00022-5

Pulit-Prociak, J., Grabowska, A., Chwastowski, J., Majka, T.M. and Banach, M. 2019. Safety of the application of nanosilver and nanogold in topical cosmetic preparations. Colloids and Surfaces B: Biointerfaces 183: 110416. https://doi.org/10.1016/j.colsurfb.2019.110416

Ragunathan, R., Velusamy, S., Nallasamy, J.L., Shanmugamoorthy, M., Johney, J., Veerasamy, S., Gopalakrishnan, D., Nithyanandham, M., Balamoorthy, D. and Velusamy, P. 2022. Synthesis and enhanced photocatalytic activity of zinc oxide-based nanoparticles and its antibacterial activity. Journal of Nanomaterials 2022(1): 3863184. https://doi.org/10.1155/2022/3863184

Rawa, A., Syahfriena, M., Mazlan, M.K.N., Ahmad, R., Nogawa, T. and Wahab, H.A. 2022. Roles of Syzygium in anti-cholinesterase, anti-diabetic, anti-inflammatory, and antioxidant: from Alzheimer's perspective. Plants 11(11): 1476. https://doi.org/10.3390/plants11111476

Reddy, N.J., Vali, N.D., Rani, M. and Rani, S.S. 2014. Evaluation of antioxidant, antibacterial and cytotoxic effects of green synthesized silver nanoparticles by Piper longum fruit. Materials Science and Engineering: C 34: 115–122. https://doi.org/10.1016/j.msec.2013.08.039

Roy, S., Hazra, B., Mandal, N. and Chaudhuri, T.K. 2013. Assessment of the antioxidant and free radical scavenging activities of methanolic extract of Diplazium esculentum. International Journal of Food Properties 16(6): 1351–1370. https://doi.org/10.1080/10942912.2011.587382

Rudrappa, M., Rudayni, H.A., Assiri, R.A., Bepari, A., Basavarajappa, D.S., Nagaraja, S.K., Chakraborty, B., Swamy, P.S., Agadi, S.N. and Niazi, S.K. 2022. Plumeria alba-mediated green synthesis of silver nanoparticles exhibits antimicrobial effect and anti-oncogenic activity against glioblastoma U118 MG cancer cell line. Nanomaterials 12(3): 493. https://doi.org/10.3390/nano12030493

Safa, M.A.T. and Koohestani, H. 2024. Green synthesis of silver nanoparticles with green tea extract from silver recycling of radiographic films. Results in Engineering 21: 101808. https://doi.org/10.1016/j.rineng.2024.101808

Sharma, A.R., Sharma, G., Nath, S. and Lee, S-S. 2024. Screening the phytochemicals in Perilla leaves and phytosynthesis of bioactive silver nanoparticles for potential antioxidant and wound-healing application. Green Processing and Synthesis 13(1): 20240050. https://doi.org/10.1515/gps-2024-0050

Sharma, V.K., Yngard, R.A. and Lin, Y. 2009. Silver nanoparticles: green synthesis and their antimicrobial activities. Advances in Colloid and Interface Science 145(1–2): 83–96. https://doi.org/10.1016/j.cis.2008.09.002

Shi, J., Xia, Y., Wang, H., Yi, Z., Zhang, R. and Zhang, X. 2022. Piperlongumine is an NLRP3 inhibitor with anti-inflammatory activity. Frontiers in Pharmacology 12: 818326. https://doi.org/10.3389/fphar.2021.818326

Siddique, M.H., Sadia, M., Muzammil, S., Saqalein, M., Ashraf, A., Hayat, S., Saba, S., Khan, A.M., Hashem, A. and Avila-Qezada, G.D. 2024. Biofabrication of copper oxide nanoparticles using Dalbergia sisso leaf extract for antibacterial, antibiofilm and antioxidant activities. Scientific Reports 14(1): 31867. https://doi.org/10.1038/s41598-024-83199-5

Sonbol, H., Ameen, F., Al Yahya, S., Almansob, A. and Alwakeel, S. 2021. Padina boryana mediated green synthesis of crystalline palladium nanoparticles as potential nanodrug against multidrug resistant bacteria and cancer cells. Scientific Reports 11(1): 5444. https://doi.org/10.1038/s41598-021-84794-6

Sukweenadhi, J., Setiawan, K.I., Avanti, C., Kartini, K., Rupa, E.J. and Yang, D-C. 2021. Scale-up of green synthesis and characterization of silver nanoparticles using ethanol extract of Plantago major L. leaf and its antibacterial potential. South African Journal of Chemical Engineering 38(1): 1–8. https://doi.org/10.1016/j.sajce.2021.06.008

Tarannum, N. and Gautam, Y.K. 2019. Facile green synthesis and applications of silver nanoparticles: a state-of-the-art review. RSC Advances 9(60): 34926–34948. https://doi.org/10.1039/C9RA04164H

Uddin, A.B.M.N., Hossain, F., Ali Reza, A.S.M., Nasrin, M.S. and Alam, A.H.M.K. 2022. Traditional uses, pharmacological activities, and phytochemical constituents of the genus *Syzygium*: a review. Food Science & Nutrition 10(6): 1789–1819. https://doi.org/10.1002/fsn3.2797

Wang, F., Niu, X., Wang, W., Jing, W., Huang, Y. and Zhang, J. 2018. Green synthesis of Pd nanoparticles via extracted polysaccharide applied to glucose detection. Journal of the Taiwan Institute of Chemical Engineers 93: 87–93. https://doi.org/10.1016/j.jtice.2018.08.022

Wang, Z. and Tang, M. 2021. Research progress on toxicity, function, and mechanism of metal oxide nanoparticles on vascular endothelial cells. Journal of Applied Toxicology 41(5): 683–700. https://doi.org/10.1002/jat.4121

Wehmas, L.C., Anders, C., Chess, J., Punnoose, A., Pereira, C.B., Greenwood, J.A. and Tanguay, R.L. 2015. Comparative metal

oxide nanoparticle toxicity using embryonic zebrafish. Toxicology Reports 2: 702–715. https://doi.org/10.1016/j.toxrep.2015.03.015

Wei, L., Lu, J., Xu, H., Patel, A., Chen, Z-S. and Chen, G. 2015. Silver nanoparticles: synthesis, properties, and therapeutic applications. Drug Discovery Today 20(5): 595–601. https://doi.org/10.1016/j.drudis.2014.11.014

Xia, G., Liu, T., Wang, Z., Hou, Y., Dong, L., Zhu, J. and Qi, J. 2016. The effect of silver nanoparticles on zebrafish embryonic development and toxicology. Artificial Cells, Nanomedicine, and Biotechnology 44(4): 1116–1121.

Yassin, M.T., Mostafa, A.A-F., Al-Askar, A.A. and Al-Otibi, F.O. 2022. Synergistic antibacterial activity of green synthesized silver nanomaterials with colistin antibiotic against multidrug-resistant bacterial pathogens. Crystals 12(8): 1057. https://doi.org/10.3390/cryst12081057

Zhang, X-F., Liu, Z-G., Shen, W. and Gurunathan, S. 2016. Silver nanoparticles: synthesis, characterization, properties, applications, and therapeutic approaches. International Journal of Molecular Sciences 17(9): 1534. https://doi.org/10.3390/ijms17091534

Zia, F., Ghafoor, N., Iqbal, M. and Mehboob, S. 2016. Green synthesis and characterization of silver nanoparticles using Cydonia oblong seed extract. Applied Nanoscience 6: 1023–1029. https://doi.org/10.1007/s13204-016-0517-z

Supplementary

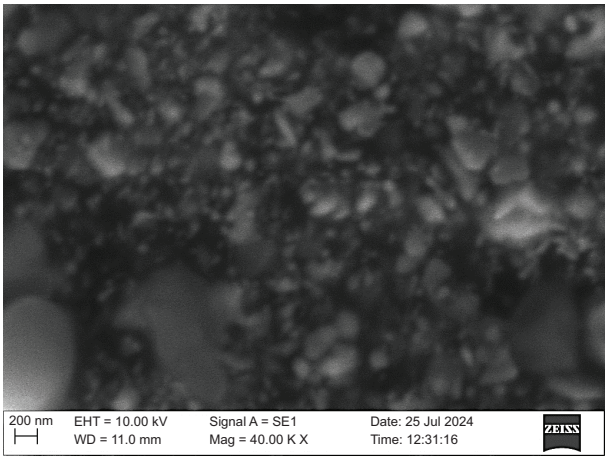

Figure S1. SEM image.

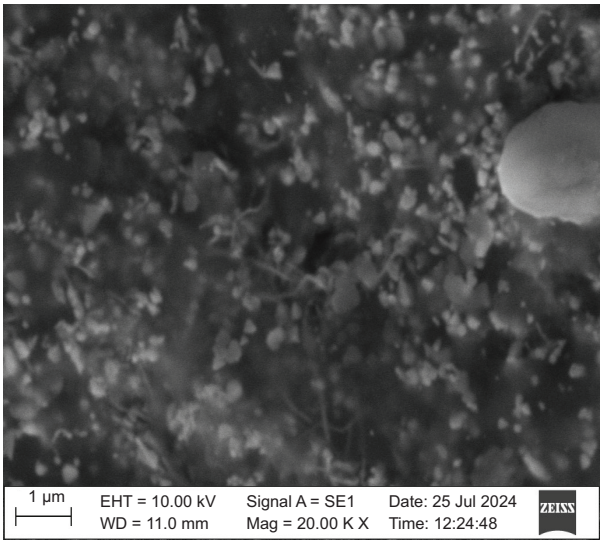

Figure S2. SEM image.

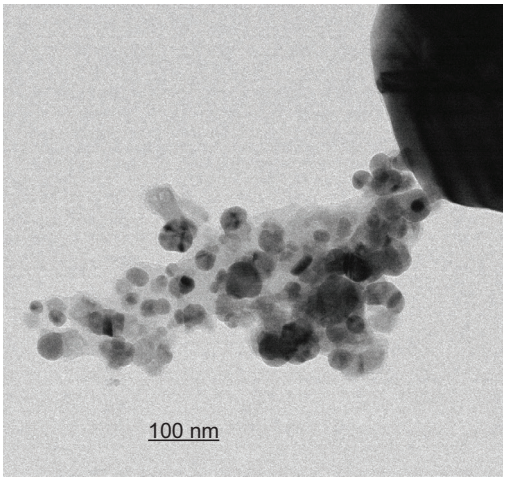

Figure S3. TEM image.

Figure S4. *Bacillus cereus*.

Figure S5. *Shigella flexneri*.